Green Synthesis of Silver Nanoparticles from De-oiled Rhizomes of *Curcuma longa* L. and Its Biomedical Potential

Sinthia Ganesan[1], Palanichamy Mehalingam[2(✉)], and Govindan Sadasivam Selvam[3]

[1] Department of Biotechnology, V.V. Vanniaperumal College for Women (Autonomous), Virudhunagar, India
[2] Research Department of Botany, V.H.N. Senthikumara Nadar College (Autonomous), Virudhunagar, India
mehalingamp@yahoo.co.in
[3] Department of Biochemistry, School of Biological Sciences, Madurai Kamaraj University, Madurai, India

Abstract. The present study deals with the synthesis of silver nanoparticles using de-oiled rhizomes of Curcuma longa aqueous extracts and its biomedical potential. Tumeric is the rhizome of Curcuma longa (Zingiberaceae) and Curcumin is extracted from it. Curcumin finds extensive use in the pharmaceutical industry. Synthesis of silver nanoparticles from 1 mM silver nitrate solution using the extract of turmeric spent was done. The colour changed from pale yellow to dark brown indicating the synthesis of silver nanoparticles. The synthesized silver nanoparticles were characterized by UV visible spectroscopy, XRD, FTIR and Zeta potential. These green synthesised silver nanoparticles were tested for antimicrobial activity by agar well diffusion method against seven human pathogenic strains such as Bacillus subtilis, Staphylococcus aureus, Streptococcus faecalis, Klebsiella pneumoniae, Pseudomonas aeruginosa, E.coli and Candida albicans. The zone of inhibition increased with increase in the concentration of silver nanoparticles in well diffusion method. Anticancer activity of silver nanoparticles was tested on breast cancer cell line, MCF-7. Cytotoxic effect was observed in tested sample concentrations after 48 h treatment. It also revealed that increase in concentration of drug showed increased cytotoxicity over the MCF-7 cell line. This efficient biomedical potential of the synthesized silver nanoparticles paves the way for its application in the area of nano-medicine.

Keywords: Anticancer activity · Antimicrobial activity · Tumeric spent · MCF-7

1 Introduction

Nanotechnology, a young science based on ancient methods is emerging as a new trend in research. Nanoparticles due to their small size have very high surface area/volume and hence more drugs can be loaded to treat several diseases, especially microbial ones.

M. Rajan et al. (Eds.): ICON 2019, SPM, pp. 94–106, 2019.
https://doi.org/10.1007/978-3-030-25135-2_10

Metal nanoparticles made of gold, silver, iron,etc. show good biomedical potential. Particularly, silver nanoparticles have been studied widely and show promise as good antimicrobial agents which can aid pharmacology [1]. The reduced size of the particles alters their physical and chemical properties drastically paving the way to newer uses in every field of science. Nanoparticles are being used in every field including optics, paint industry, environmental protection, water purifiers and electronic industry [2]. Silver nanoparticles have excellent antimicrobial activity, thermoplasmonic capabilities, and superior surface Raman properties.

Tumeric (*Curcuma longa L.*) (Fig. 1) a monocot, is a well-known anti-bacterial and anti-cancer agent belonging to the *Zingiberaceae* family. It has been used in ayurvedic medicines since time immemorial. Turmeric is extensively used as a spice, food preservative and colouring material in India, China and South East Asia. It has been used in traditional medicine as a household remedy for various diseases, including the common cold, biliary disorders, anorexia, cough, diabetic wounds, hepatic disorders, rheumatism, sinusitis and as a antibiotic.

Fig. 1. *Curcuma longa* L.

Curcumin (diferuloylmethane), the main yellow bioactive component of turmeric, has been shown to have a wide range of biological actions which include its antiinflammatory, antioxidant, anticarcinogenic, antimutagenic, anticoagulant, antifertility, antidiabetic, antimicrobial, antifibrotic, antivenom, antiulcer and antifat activities. Its anticancer effect is mainly mediated through induction of cell death or apoptosis. Its antiinflammatory, anticancer and antioxidant roles have been used by many to control rheumatism, carcinogenesis and oxidative stress-related problems. Curcumin has already been used clinically to reduce post-operative inflammation [3].

There are many methods used for the production of silver nanoparticles (AgNPs) which include chemical [4], electrochemical [5], radiation [6], photochemical methods [7], Langmuir-Blodgett [8, 9] and biological techniques [10]. Biological synthesis is far superior as it offers several advantages which include rapid synthesis, high yields and more importantly, the lack of costly downstream processing required to produce the particles [11–13]. Biological methods include the use of plants or microbes as reducing agents. Of these, green synthesis of silver nanoparticle using plants is considered best

for the rapid production of large quantities of silver nanoparticles to successfully meet the growing needs and current market demand and simultaneously maintain a cleaner and safer environment for humans [14]. The biological route using plants is very fast, cost effective, environment friendly and non-toxic. Plants can function as both reducing and stabilizing agents and surpass microbial methods by bypassing the complicated process of maintaining cultures. Large scale production of commercial and economic nanoparticles is feasible by using easily available plant extracts. There are several studies that report on the use of plant extracts in nanoparticle synthesis [15].

For the last few decades, extensive work has been done to establish the biological activities and pharmacological actions of turmeric and its extracts. The essential oil, Curcumin, is extracted from turmeric and has high medicinal value. The de-oiled turmeric is an industrial waste and adulterant. The present study is directed towards the efficient synthesis and characterization of silver nanoparticles using aqueous extracts of de-oiled *Curcuma longa* and the study of its biomedical potential as an antimicrobial and anticancer drug.

2 Materials and Methods

2.1 Materials

De-oiled *Curcuma longa* (Fig. 2) was supplied by ***Synthite,*** the world's largest producer of value added spice extracts and natural spice powder. All the reagents purchased were of analytical grade and used without any further purification. Silver nitrate ($AgNO_3$) was purchased from Sigma-Aldrich from India. The bacterial strains were purchased from Gandhigram Rural Institute - Deemed University, Gandhigram. Mueller–Hinton broth and agar were purchased from Hi-Media, Mumbai, India. Double distilled water was used throughout the experiments.

Fig. 2. De-oiled *Curcuma longa* L.

2.2 Preparation of Extracts

The de-oiled turmeric sample was air dried and stored in the refrigerator. About 10 g of sample material was mixed with 100 ml of deionised water and added into a 500 ml beaker. The mixture was heated at 60 °C for 15 min. After that the solution was filtered with the help of Whatman No. 1 filter paper. Then the de-oiled turmeric aqueous extract (Fig. 3) was kept in refrigerator at 4 °C for future experiments.

Fig. 3. De-oiled *Curcuma longa* extract

2.3 Synthesis of AgNPs

For the reduction of silver ions, 90 ml of 1 mM AgNO3 aqueous solution of silver nitrate was taken in Erlenmeyer flask, and 10 ml of de-oiled turmeric sample extract was added to it separately at room temperature. After 30 min the solution turned pale yellow to dark brown indicating the formation of silver nanoparticles.

3 Characterization of AgNPs

The optical properties of the synthesized silver nanoparticles were studied using UV–vis spectroscopy (UV-1800v, Shimadzu, Japan). The surface morphology and size of the synthesized silver nanoparticles was analysed by using particle size analyser. The FTIR spectrum of synthesized silver nanoparticles was analysed with a Thermo Scientific Nicolet 380 FT-IR Spectrometer by KBr pellet method. The percentage presence of silver ions from the synthesized silver nanoparticles was done by using energy dispersive X-ray spectrum (EDX). The synthesized metallic nanoparticles was analysed by using X-ray diffractometer model (Shimadzu, Japan) with 40 kV, 30 mA with Cu k a radiation at 2θ angle.

4 Antimicrobial Activity

The antimicrobial activity was done using human pathogenic bacteria (*Bacillus subtilis*, *Staphylococcus aureus*, *Streptococcus faecalis, Klebsiella pneumoniae*, *Pseudomonas aeruginosa, E.coli*, *Candida albicans*) by agar well diffusion method. Muller Hinton agar medium was used to sub culture bacteria which were incubated at 37 °C for 24 h. Then the overnight inoculated cultures were taken and spread on the Muller Hinton agar plates. Wells were formed by using a cork borer of 6 mm diameter. Plant extract, silver nitrate and different concentration of AgNPs (100 µg/ml, 150 µg/ml, 200 µg/ml) were poured into each well. The streptomycin (20 µg/ml) was used as a control. The antimicrobial activity of AgNPs was determined by measuring the zone of inhibition around the well diameter (in mm) with the help of scale and the results were tabulated.

5 Anticancer Study

5.1 Preparation of Cell Suspension

For this study, the MCF-7cell lines were procured from National Centre for Cell Science (NCCS), Pune, India. A subculture of MCF 7 cells in Dulbecco's Modified Eagle's Medium (DMEM) was trypsinized separately. After discarding the culture medium, to the disaggregated cells in the flask, 25 ml of DMEM with 10% FCS was added. The cells were suspended in the medium by gentle passage with a pipette and the cells were homogenized.

5.2 Seeding of Cells

One ml of the homogenized cell suspension was added to each well of a 24 well culture plate along with different concentration of samples (3.12 to 400 µg/ml) and incubated at 37 °C in a humidified CO_2 incubator with 5% CO_2. After 48 h incubation the cells were observed under an inverted tissue culture microscope. With 80% confluence of cells, cytotoxicity assay was carried out.

5.3 Cytotoxicity Assay

The assay was carried out using (3- (4, 5- dimethyl thiazol-2yl)- 2, 5- diphenyltetrazolium bromide (MTT). MTT is cleaved by mitochondrial Succinate dehydrogenase and reductase of viable cells, yielding a measurable purple product formazan. This formazan production is directly proportional to the viable cell number and inversely proportional to the degree of cytotoxicity. After 48 h incubation, the wells were treated with MTT and left for 3 h at room temperature. The content of all the wells was removed using micropipette and 100 µl SDS in DMSO was added to dissolve the formazan crystals. Absorbance's were read using Read Well Touch micro plate reader at 570 nm [16].

6 Results and Discussion

On addition of de-oiled turmeric water extract to silver nitrate solution, a pale yellow solution was formed. The colour of the solution changed gradually from pale yellow to dark brown (Fig. 4) indicating the formation of silver nanoparticles. The colour change was immediate when exposed to sunlight and slow when kept in the dark indicating the catalytic role of sunlight which assists the formation of silver nanoparticles.

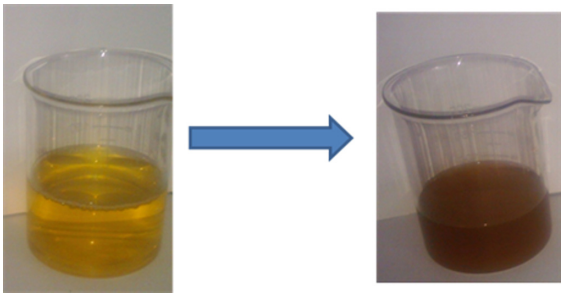

Fig. 4. Colour changes from yellow to brown on adding silver nitrate

6.1 Characterisation of Silver Nanoparticles

Optical Properties: The synthesized silver nanoparticles were characterized by **UV visible spectroscopy** to confirm the synthesis of silver nanoparticles. Due to surface Plasmon resonance of silver nanoparticles, a peak at 400–420 nm confirms the presence of silver. Two peaks were formed, one at 697 nm (1 in Fig. 5) and another at 417.5 nm (2 in Fig. 5). The peak at 417.5 nm corresponds to silver nanoparticles.

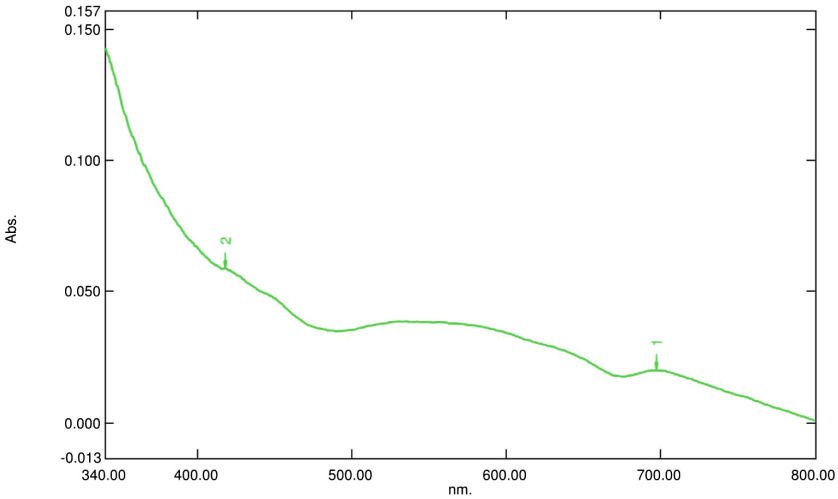

Fig. 5. UV spectra- peak 2 at 417.5 nm indicates AgNPs

FTIR Analysis: Fourier Transform Infra Red Spectroscopy was carried out to identify the groups responsible for reduction and stabilization of the synthesized silver nanoparticles. The FTIR spectrum (Fig. 6) showed four strong peaks at 3443.66 cm^{-1}, 1604.66 cm^{-1}, 1379.97 cm^{-1} and 1076.21 cm^{-1} and several smaller peaks at 775.33 cm^{-1}, 1745.46 cm^{-1}, 2926.78 cm^{-1}, 2313.46 cm^{-1}, 1311.50 cm^{-1}, 1229.54 cm^{-1}, 825.48 cm^{-1}, 775.33 cm^{-1} and 518.82 cm^{-1}. The highest absorbance at 3443.66 cm^{-1} corresponds to O-H stretch of carboxylic acids, phenols and alcohols; the second peak at 2926.78 cm^{-1} is assigned to the C-H stretch of alkanes; The peak at 1745.46 cm^{-1} indicates C = O stretch of aldehydes; 1604.66 cm^{-1} peak shows the presence of amides (N-H bend); The second highest peak at 1379.97 is for alkanes; 1311.50 cm^{-1} shows N-O stretch of nitro compounds; 1229.54 cm^{-1} corresponds to ethers(C-O-C); 1076.21 cm^{-1} to C-N stretch of aliphatic amines; peaks 825.48 cm^{-1} and 775.33 cm^{-1} correspond to aromatic p- and m- disubstituted compounds and 518.82 cm^{-1} corresponds to alkyl halides (C-Br stretch).

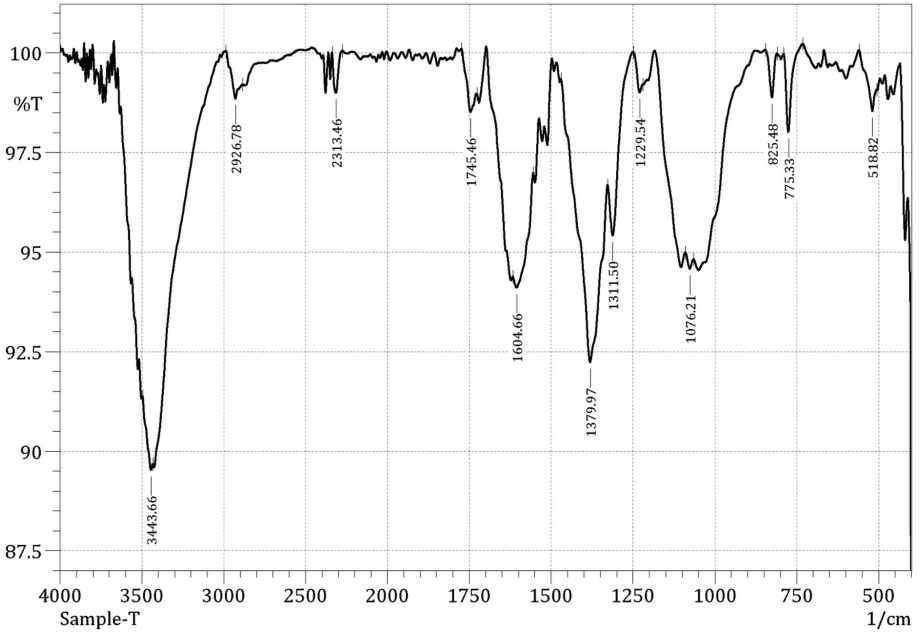

Fig. 6. FTIR spectra indicates presence of phenols

XRD Studies: X-Ray Diffraction studies were carried out with the synthesized silver nanoparticles to elucidate their crystalline structure. Crystal size was calculated using Debye-Scherrer equation. The equation can be written as:

$$\tau = K\lambda/\beta\cos\theta$$

where:

- τ is the mean size of the ordered (crystalline) domains, which may be smaller or equal to the grain size
- K is a dimensionless **shape factor**, with a value close to unity. The shape factor has a typical value of about 0.9, but varies with the actual shape of the crystallite
- λ is the X-ray wavelength
- β is the line broadening at half the maximum intensity (FWHM), after subtracting the instrumental line broadening, in radians. This quantity is also sometimes denoted as 2θ
- θ is the Bragg angle.

The average crystal size was calculated, using Scherrer-Debye's equation for FWHM and 2 theta values (Table 1), as **19.8 nm**.

Table 1. XRD analysis 2 theta values

Pos. [°2Th.]	Height [cts]	FWHM left [°2Th.]	d-spacing [Å]	Rel. Int. [%]
27.9692	48.66	0.2952	3.19016	51.33
32.3391	94.80	0.2460	2.76837	100.00
46.3627	65.06	0.3936	1.95847	68.63
54.8643	23.68	0.3936	1.67341	24.98
57.6923	16.87	0.5904	1.59793	17.80
67.5890	8.13	1.1808	1.38604	8.58
76.8832	15.86	1.1808	1.24001	16.73

The XRD graph (Fig. 7) shows major peaks at 2 theta values of 32.34, 46.36 and 76.88. The crystal structure was determined by comparing d-spacing values with standard data using JCPDF software. The crystal structure matched PDF #411402 for silver showing Hexagonal structure at planes 1.386 (112) and 1.2400 (201).

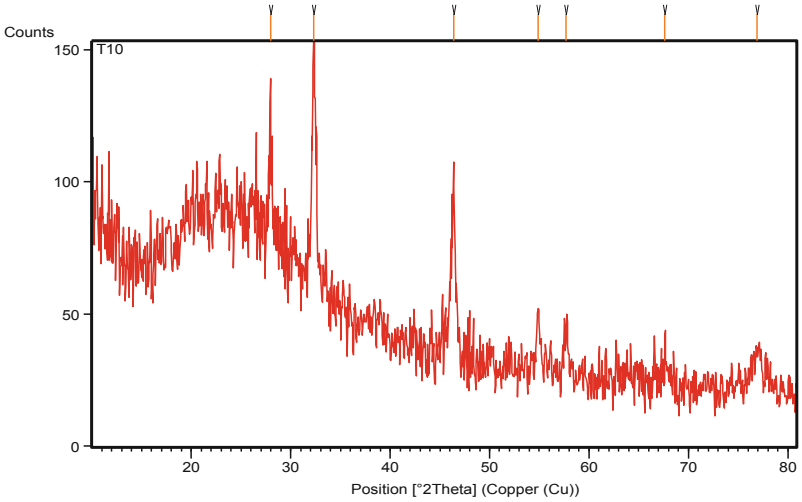

Fig. 7. XRD graph revealed hexagonal structure

Particle Size Analysis: The size of the synthesised nanoparticles was +measured using a Flow cell (Shimadzu SALD-2300). The size of the particles varies from 25 nm-75 nm with an average size of around 50 nm (Fig. 8).

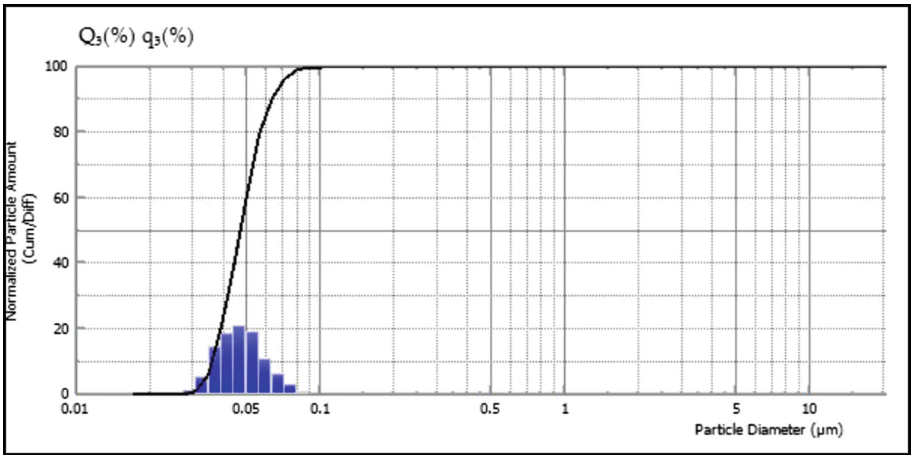

Fig. 8. Particle size analysis

6.2 Biomedical Potential

Antimicrobial Activity. The antimicrobial activity of silver nanoparticles against human pathogenic bacteria is mostly used in the medical field to hasten wound healing and also in water purification. The synthesized AgNPs were treated against seven bacterial strains: Gram positive bacteria such as *Bacillus subtilis*, *Staphylococcus*

aureus, *Streptococcus faecalis* and Gram negative bacteria *Klebsiella pneumoniae*, *Pseudomonas aeruginosa, E.coli* and a fungus *Candida albicans*. Agar well diffusion method was used (Fig. 9).

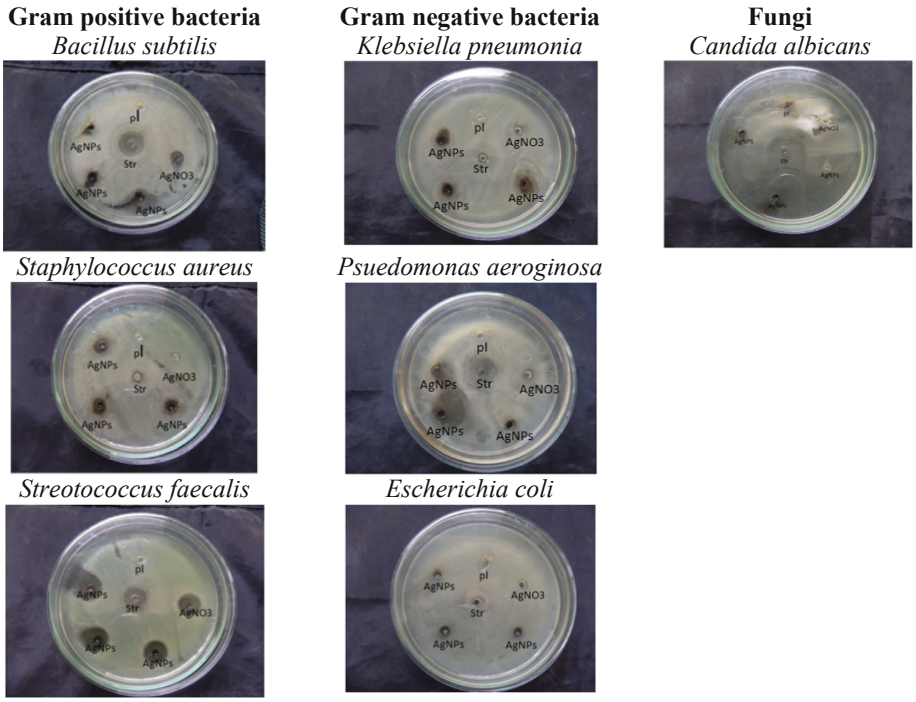

Fig. 9. Antimicrobial activity by well diffusion method

The zones of inhibition (Table 2) illustrated that the maximum zone of inhibition was against (*Bacillus subtilis* 13 mm) and (*Pseudomonas aeruginosa 13* mm) respectively. The ZOI increased with increase in concentration of AgNPs. The

Table 2. Zone of inhibition (ZOI) in mm

S. No	Cultures	Plant extract	AgNO3 (100 µl)	AgNPs (100 µl)	AgNPs (200 µl)	AgNPs (300 µl)	Streptomycin
1	*Bacillus subtilis*	10	25	12	13	15	30
2	*Staphylococcus aureus*	12	22	13	17	19	25
3	*Streptococcus faecalis*	10	27	25	28	29	30
4	*Klebsiella pneumoniae*	10	30	15	18	20	31
5	*Pseudomonas aeruginosa*	12	35	22	23	24	20
6	*Escherichia coli*	10	27	16	18	19	32
7	*Candida albicans*	11	35	12	13	18	45

remaining bacterial strains were only fairly susceptible. The synthesized AgNPs exhibited significant antimicrobial activity against human pathogenic bacteria.

Cytotoxicity. The in-vitro cytotoxicity activity studies proved that MCF 7 cells were reduced significantly with increase in AgNPs concentration (Table 3). In the cell line, cytotoxic effect was observed in turmeric spent AgNPs concentration after 48 h treatment. It also revealed that increased concentration of AgNPs shown increased cytotoxicity over the MCF 7 cell line.

Table 3. MTTP assay for cytotoxicity

Conc of AgNPs	OD	OD (after 48 h)	Cell viablity
0	1.325	1.325	100.00
3.12	1.175	1.325	88.68
6.25	0.963	1.325	72.68
12.5	0.914	1.325	68.98
25	0.867	1.325	65.43
50	0.754	1.325	56.91
100	0.675	1.325	50.94
200	0.641	1.325	48.38

From the graph (Fig. 10) the IC 50 value was calculated as 1.84 showing that the nanoparticles showed good efficacy in destroying cancer cells.

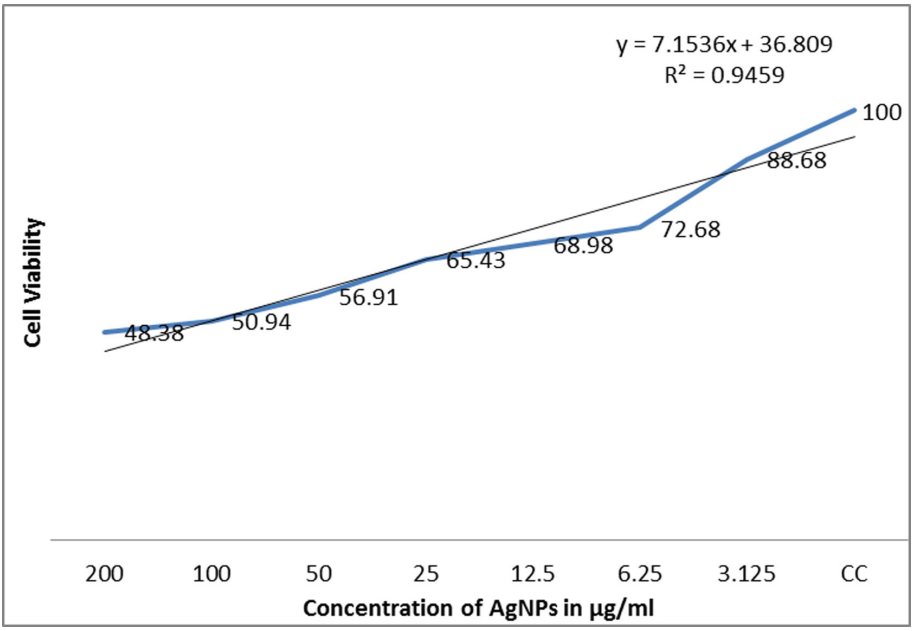

Fig. 10. MTTP assay for cytotoxicity

The cells were observed under an inverted tissue culture microscope (Fig. 11). The increase in concentration of AgNPs resulted in increase in cytotoxicity.

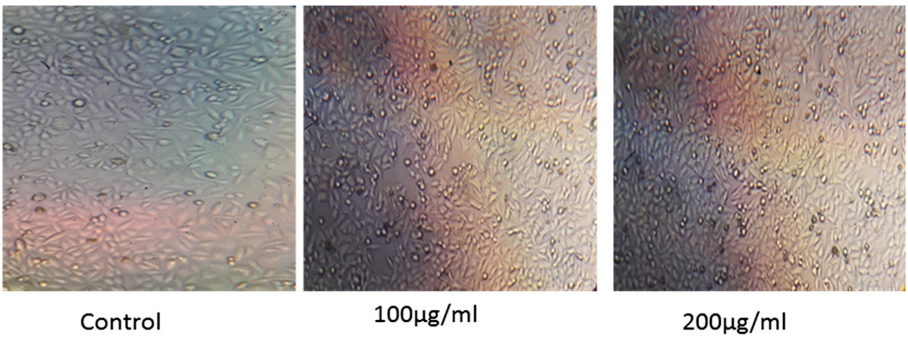

Fig. 11. MCF-7 treated with de-oiled turmeric AgNPs

7 Conclusion

The active ingredients in turmeric like curcumin and turmerone are not the only contents in turmeric that have medicinal value. Even the de-oiled turmeric devoid of turmerone and curcumin shows biomedical potential.

Silver nanoparticles were produced using de-oiled tumeric as reducing and capping agent in the presence of sunlight. They were characterised by UV-vis, FTIR, XRD and particle size analyser. Hexagonal silver nanoparticles of size around 40 nm, stabilized by phenol groups were obtained. The silver nanoparticles showed good antimicrobial activity against selected bacteria and fungi. The activity increased with increase in concentration of nanoparticles. Excellent activity against *Streptococcus faecalis* was seen comparable to Streptomycin. Cytotoxic effect was observed in tested sample concentrations after 48 h treatment. It also revealed that increase in concentration of drug showed increased cytotoxicity over the MCF-7 cell line with an effective IC 50 value of 1.84. This efficient biomedical potential of the synthesized silver nanoparticles paves the way for its application in the area of nano-medicine.

References

1. Rai, M., et al.: Synergistic antimicrobial potential of essential oils in combination with nanoparticles: emerging trends and future perspectives. Int. J. Pharm. **519**, 67–78 (2017)
2. Azizinezhad, F., et al.: Synthesis of the silver nanoparticles with the using of camomile plant. Eur. J. Exp. Bio. **4**(2), 124–127 (2014)
3. Chattopadhyay, I., Biswas, K., Bandyopadhyay, U., Banerjee, R.K.: Turmeric and curcumin: biological actions and medicinal applications. Curr. Sci. **87**(1), 46 (2004)

4. Sun, Y., Yin, Y., Mayers, B.T., Herricks, T., Xia, Y.: Uniform form silver nanowires synthesis by reducing $AgNO_3$ with ethylene glycol in presence of seeds and polyvinyl pyrrolidone. Chem. Mater. **14**, 4736–4745 (2002)
5. Yin, B., Ma, H., Wang, S., Chen, S.: Electrochemical synthesis of silver nanoparticles under protection of poly N-vinyl pyrrolidone. J. Phys. Chem. B **107**, 8898–8904 (2003)
6. Dimitrijevic, N.M., Bartels, D.M., Jonah, C.D., Takahashi, K., Rajh, T.: Radiolytically induced formation and optical absorption spectra of colloidal silver nanoparticles in supercritical ethane. J. Phys. Chem. B **105**, 954–959 (2001)
7. Callegari, A., Tonti, D., Chergui, M.: Photochemically grown silver nanoparticles with wavelength-controlled size and shape. Nano Lett. **3**, 1565–1568 (2003)
8. Zhang, L., Shen, Y.H., Xie, A.J., Li, S.K., Jin, B.K., Zhang, Q.F.: One-step synthesis of monodisperse silver nanoparticles beneath vitamin E Langmuir monolayers. J. Phys. Chem. B **110**, 6615–6620 (2006)
9. Swami, A., Selvakannan, P.R., Pasricha, R., Sastry, M.: One-step synthesis of ordered two dimensional assemblies of silver nanoparticles by the spontaneous reduction of silver ions by pentadecylphenol Langmuir monolayers. J. Phys. Chem. B **108**, 19269 (2004)
10. Naik, R.R., Stringer, S.J., Agarwal, G., Jones, S., Stone, M.O.: Biomimetic synthesis and patterning of silver nanoparticles. Nat. Mater. **1**, 169–172 (2002)
11. Gannimani, R., Perumal, A., Krishna, S., Sershen, M., Mishra, A., Govender, P.: Dig. J. Nanomater. Biostruct. **9**, 1669 (2014)
12. Das, V.L., Thomas, R., Varghese, R.T., Soniya, E., Mathew, J., Radhakrishnan, E.: 3 Biotech. **4**, 121 (2014)
13. Liu, B., Xie, J., Lee, J., Ting, Y., Chen, J.P.: Green synthesis of silver nanoparticles from Moringa oleifera leaf extracts and its antimicrobial potential. J. Phys. Chem. B **109**, 15256 (2005)
14. Banerjee, P., Satapathy, M., Mukhopahayay, A., Das, P.: Leaf extract mediated green synthesis of silver nanoparticles from widely available Indian plants: synthesis, characterization, antimicrobial property and toxicity analysis. Bioresour. Bioprocess. **1**, 3 (2014)
15. Moodley, J.S., Krishna, S.B.N., Pillay, K., Sershen, M., Govender, P.: School Advances in natural sciences: nanoscience and nanotechnology, vol. 9, p. 015011 (9pp) (2018)
16. Mosman, T.: Rapid colorimetric assay for cellular growth and survival, application to proliferation and cytotoxicity assays. J. Immunol. Methods **65**, 55–63 (1983)